RESTRICTED

COPY NO.
RM No. E8G02c

UNCLASSIFIED

NACA

RESEARCH MEMORANDUM

INVESTIGATION OF THE I-40 JET-PROPULSION ENGINE IN THE CLEVELAND ALTITUDE WIND TUNNEL

IV - ANALYSIS OF COMBUSTION-CHAMBER PERFORMANCE

By Reece V. Hensley

Flight Propulsion Research Laboratory
Cleveland, Ohio

NATIONAL ADVISORY COMMITTEE FOR AERONAUTICS

WASHINGTON
August 25, 1948

RESTRICTED

UNCLASSIFIED

NATIONAL ADVISORY COMMITTEE FOR AERONAUTICS

RESEARCH MEMORANDUM

INVESTIGATION OF THE I-40 JET-PROPULSION ENGINE IN THE CLEVELAND ALTITUDE WIND TUNNEL

IV - ANALYSIS OF COMBUSTION-CHAMBER PERFORMANCE

By Reece V. Hensley

SUMMARY

Combustion-chamber performance characteristics of the I-40 jet-propulsion engine were determined from an investigation of the complete engine installed in an airplane fuselage in the Cleveland altitude wind tunnel over a range of ram pressure ratios from 0.98 to 1.76. The standard type C combustion chamber and a modified type E combustion chamber were investigated.

The combustion-chamber performance characteristics are presented as functions of the engine speed corrected to NACA standard sea-level inlet conditions. The effect of variations in altitude and ram pressure ratio on combustion efficiency and on combustion-chamber pressure losses is presented. The decrease in engine-cycle efficiency due to combustion-chamber pressure losses is evaluated.

Combustion efficiency varied directly with the ram pressure ratio and engine speed and inversely with the altitude. The combustion efficiency was generally higher for the type C combustion chamber than for type E. Pressure losses of about 6 percent of the combustion-chamber-inlet total pressure were obtained with the type C combustion chamber and slightly lower losses were encountered with the type E combustion chamber. Percentage losses in total pressure were inappreciably affected by changes in altitude or ram pressure ratio up to a value of 1.3. At rated engine speed, the decrease in engine-cycle efficiency due to combustion-chamber pressure losses was slight; the fractional loss varied inversely as the engine speed, generally reaching a value of one-half the engine-cycle efficiency attained at a corrected engine speed between 6000 and 8000 rpm.

INTRODUCTION

An investigation under simulated flight conditions of the performance of the I-40 engine installed in an airplane fuselage has been conducted in the Cleveland altitude wind tunnel. The performance and operational characteristics of the component parts of the I-40 jet-propulsion engine installed in this airplane were determined in addition to the evaluation of the over-all characteristics. Reference 1 summarizes the over-all engine-performance and windmilling drag characteristics of the unit and references 2 and 3 present the performance characteristics of the compressor and the turbine, respectively, as determined from the investigation of the complete engine.

An analysis of the performance of the combustion chamber, including a comparison of the performance of the standard type C and a modified type E (manufacturer's designation), is presented. For the flight conditions simulated, data are presented for both the type C and the type E combustion chambers that show the combustion-chamber efficiency, the losses in total pressure occurring in the combustion chamber, and the effect of these pressure losses on the engine-cycle efficiency.

Operating characteristics of the combustion chambers could be obtained only at conditions permitted by the over-all performance limits of the engine at each set of simulated flight conditions. The engine was operated from approximately static conditions to a ram pressure ratio (defined as the ratio of the total pressure at the compressor inlet to the tunnel static pressure) of 1.76 and at simulated altitudes from 10,000 to 50,000 feet. For all conditions except the low ram pressure ratios at simulated altitudes of 30,000 feet and higher, corresponding NACA standard temperatures were maintained. At low ram pressure ratios in combination with the higher altitudes, temperatures were as much as 30° F above the corresponding standard temperatures because of the limited refrigerated-air supply available.

DESCRIPTION OF COMBUSTION CHAMBERS

The combustion section of the I-40 jet-propulsion engine consists of 14 individual combustion chambers. Air enters the combustion chamber from the periphery of the centrifugal compressor through air adapters. The combustion chamber has a circular cross section and a decreasing area in the direction of the gas flow. Each chamber contains a removable perforated combustion liner (fig. 1) that

divides the combustion zone from the passage for the secondary air flow. The circular cross-sectional area of the liner increases slightly in the direction of the flow. The downstream end of the liner is a truncated cone that fits the tapered combustion chamber; the upstream end is closed by a hemispherical dome. A fuel nozzle that directs the fuel spray downstream along the combustion-chamber axis is located in the center of each dome. Ignition is provided by spark plugs in two of the 14 liner domes. The other combustion chambers are lighted by cross-ignition passages, which interconnect all the chambers.

In the type C combustion chamber, the dome has louvers near its center to admit primary air to the combustion zone. These louvers give the primary air a swirling motion. The type C dome is removable and is attached inside the combustion chamber by brackets. A 40-gallon-per-hour Monarch fuel nozzle with an 80° spray cone was used with the standard type C combustion chamber.

The type E combustion chamber differs primarily from the standard type C chamber in the design of the liner dome. The type E dome has louvers only near its periphery for the admittance of air to the combustion zone. With this arrangement, the air must reverse the direction of its flow in passing through the louvers in order to reach the primary combustion region in the center of the dome. The dome is of smaller diameter than the liner to provide an auxiliary annular slot for air flow between the two parts. This design was adopted to lessen the deposition of carbon on the combustion liner. In the type E combustion chamber, the standard type C liner was used but slight alterations were made at the upstream end in order to facilitate integral welding of the dome and the liner that was used instead of the bracket mounting used with the type C combustion chamber.

The fuel system of the engine configuration with the type E combustion chambers also differed in several respects from the standard fuel system. A 30-gallon-per-hour Monarch nozzle with a spray-cone angle of 60° was used. A single fuel-metering valve controlled the fuel flow to all combustion chambers; whereas the fuel was metered individually by each of the nozzles in the standard fuel system. This valve was spring-loaded to insure a certain minimum opening pressure for the low fuel-flow range. This change in fuel systems may have resulted in an irregular distribution of fuel flows among the individual combustion chambers at low fuel flows when the difference in the pressure of the fuel in the lines for the top

and bottom units may have been large enough relative to the fuel-line pressure to make the fuel-delivery characteristics of the individual nozzles dissimilar.

ENGINE INSTALLATION AND INSTRUMENTATION

A detailed description of the installation of the airplane fuselage in the altitude wind tunnel and of the instrumentation of the I-40 jet-propulsion engine installed in the plane is given in reference 1. The outer sections of the wings were removed in order that the resulting configuration would span the test section of the tunnel; otherwise the airplane as mounted in the tunnel essentially duplicated the flight configuration. A Y-shaped ram pipe was installed to introduce air at greater-than-tunnel pressures to the inlet ducts when conditions other than static operation were simulated.

The stations at which instrumentation was installed are shown in figure 2. This report is mainly concerned with stations 2 (compressor inlet), 4(combustion-chamber inlet), 5(combustion-chamber outlet), 7(calibration ring), and 8(tail-pipe-nozzle outlet rake). Measurements at station 7 or 8 are necessary to determine the state of the gas after combustion; those at station 8 were used when available, but with the type E combustion chamber no measurements at station 8 were obtained.

At the combustion-chamber inlet (station 4), temperature and total-pressure measurements were made in three of the 14 individual chambers that make up the combustion section. These measurements were made by using three rakes, each of which contained five total-pressure tubes and four thermocouples equally spaced and alternately located. The rakes spanned the air adapters in a direction approximately perpendicular to the engine radius. The plane of measurement was located 3.75 inches downstream of the trailing edge of the inner vane in the compressor-outlet elbow.

At station 5 the combustion-chamber-outlet total pressure was measured by single total-pressure tubes located in three of the chambers. The tubes were located 1.68 inches from the outside surface of the combustion chambers and were circumferentially displaced 0.95 inch from the engine radii bisecting the combustion-chamber outlets. The plane of measurement was 1.10 inches upstream of the end of the combustion-chamber liners. Thermocouples installed to indicate which units were lighted were located in each of the combustion-chamber outlets. Because these thermocouples were

subjected to radiation from the hot gases in the primary combustion zone, the readings were unsuitable for performance calculations.

The calibration ring (station 7) was mounted between the exhaust cone and the tail pipe. The temperature at this point was obtained by 14 equally spaced thermocouples extending 1.47 inches into the gas stream. The total pressure was given by two diametrically opposite total-pressure tubes extending 2.00 inches into the gas stream. Two diametrically opposite pressure orifices were used to measure the static pressure.

The plane of measurement of the tail-pipe-nozzle outlet rake (station 8) was located 1 inch inside the tail pipe. At this station sufficient static-pressure tubes and orifices, total-pressure tubes, and thermocouples were installed for an accurate determination of the state of the gas flow at the outlet of the tail-pipe nozzle. Details of the instrumentation at this station are given in reference 3.

SYMBOLS

The symbols used in this report are as follows:

A	cross-sectional area, square feet
C	gas-flow calibration constant for use with calibration-ring measurements
c_p	specific heat at constant pressure, Btu per pound $^{\circ}F$
g	acceleration due to gravity, 32.17 feet per second per second
K	combustion-chamber friction pressure-loss factor
k	gas-flow calibration factor for tail-pipe-nozzle outlet rake
M	Mach number, ratio of gas speed to local speed of sound
N	rotational speed of engine, rpm
P	total pressure, pounds per square foot absolute
ΔP_F	loss in total pressure in combustion chamber due to friction, pounds per square foot
ΔP_M	loss in total pressure in combustion chamber due to addition of heat to the air flowing through the combustion chamber (momentum pressure loss), pounds per square foot

ΔP_T over-all loss in total pressure in combustion chamber due to friction and heat addition, pounds per square foot

p static pressure, pounds per square foot absolute

R gas constant, foot-pounds per pound $^{\circ}R$

T total temperature, $^{\circ}R$

T_i indicated temperature, $^{\circ}R$

t static temperature, $^{\circ}R$

W air mass flow through each combustion chamber, pounds per second

W_a air mass flow through engine, pounds per second

W_f fuel mass flow through engine, pounds per second

W_g gas mass flow through engine, pounds per second

α thermocouple impact-recovery factor

γ ratio of specific heat at constant pressure to specific heat at constant volume

θ temperature correction factor, ratio of compressor inlet-air total temperature to NACA standard sea-level static temperature

η engine-cycle efficiency

η_b combustion-chamber efficiency

Subscripts:

0 free stream

2 compressor inlet (average of front and rear inlets)

4 combustion-chamber inlet

5 combustion-chamber outlet

7 calibration ring at juncture of exhaust cone and tail pipe

8 tail-pipe-nozzle outlet rake

9 vena contracta in jet from tail-pipe nozzle

B entrance to combustion zone of equivalent combustion chamber of constant area

b combustion chamber

j average between station 9 and free stream

s tail-pipe-nozzle outlet shell

x annular increment of area in tail-pipe-nozzle outlet

METHODS OF CALCULATION

Temperatures. - Static temperatures were obtained from indicated temperature readings by

$$t = \frac{T_i}{1 + \alpha\left[\left(\frac{p}{p}\right)^{\frac{\gamma-1}{\gamma}} - 1\right]}$$

Calibrations of thermocouples of the type used in these investigations gave 0.86 as the value of α. The total temperatures were obtained from these calculated values of the static temperature by applying the isentropic relation

$$\frac{T}{t} = \left(\frac{p}{p}\right)^{\frac{\gamma-1}{\gamma}}$$

Because the conditions of the air stream at the compressor inlet (station 2), rather than at the entrance of the airplane duct system were used to establish the simulated flight conditions and all ducting losses were thus left out of the engine computations, the static temperature t_0 corresponding to the compressor-inlet conditions had to be calculated. The isentropic relation

$$t_0 = T_2\left(\frac{p_0}{p_2}\right)^{\frac{\gamma-1}{\gamma}}$$

was used. Inasmuch as the tail-pipe-nozzle outlet static pressure was greater than the tunnel static pressure p_0, the temperature of the exhaust gas at the tunnel static pressure t_9 was obtained in a similar manner from the equation

$$t_9 = t_8 \left(\frac{p_0}{p_8}\right)^{\frac{\gamma-1}{\gamma}}$$

Because the thermocouples at station 5 were subjected to radiation from the primary combustion zone, they were unsatisfactory for the determination of the combustion-chamber-outlet temperature. As a result, T_5 was calculated from temperature measurements made downstream of the turbine: For the type C combustion-chamber, temperature readings at the tail-pipe-nozzle outlet rake (station 8) were used and, for the type E combustion chamber, the temperature measurements at the calibration ring (station 7) were necessarily used owing to the absence of the tail-pipe-nozzle outlet rake during these tests. In the determination of the combustion-chamber-outlet temperature in this manner, the enthalpy drop across the turbine was assumed equal to the measured enthalpy rise across the compressor. The tail-pipe-nozzle outlet total temperature T_8 (or the calibration-ring total temperature T_7) and the turbine enthalpy change were then used to obtain T_5 by use of the charts of reference 4. The value of T_5 obtained by this method was slightly low because of the neglect of mechanical-friction losses and of radiation between station 5 and the downstream measuring station used in the calculation.

Specific heats and ratio of specific heats. - For all locations downstream of the point at which fuel was injected, the values of c_p and γ used in the calculations were obtained from a chart relating these quantities to the temperature and fuel-air ratio. The values used in preparing the chart were weighted averages of the values for the various constituents of the exhaust gas obtained with an assumed combustion efficiency of 98 percent. The chart was developed for a fuel having a hydrogen-carbon ratio of 0.170. Measured values of the fuel-air ratio and the average value of the temperature for the part of the cycle under consideration were used in conjunction with the chart in the determination of c_p and γ.

Gas flow and air flow. - For the data presented for the type C combustion chamber, the gas flow was determined from tail-pipe-nozzle outlet measurements. Because of the variation of the pressures and temperatures across the tail pipe at the plane of measurement, the total area was divided into a series of annuli and the

gas flow through each annulus was calculated. The value of the total gas flow through the engine, taken as the summation of these incremental values, was given by the following equation (derived in reference 1):

$$W_g = \left\{ k\, p_8 \sqrt{\frac{2\gamma g}{(\gamma - 1)R}} \sum A_x \sqrt{\frac{\left[\left(\frac{p_x}{p_x}\right)^{\frac{\gamma-1}{\gamma}} - 1\right] + \alpha\left[\left(\frac{p_x}{p_x}\right)^{\frac{\gamma-1}{\gamma}} - 1\right]^2}{T_{i,x}}} \right\} Y$$

where

$$Y = 1 + 1.8 \times 10^{-5} (T_s - 520)$$

For use in this equation, R was assumed constant and equal to 53.86. In this equation Y is a temperature-correction factor to account for the change in area of the tail-pipe-nozzle outlet with the temperatures encountered during operation.

When the calibration-ring measurements had to be used to obtain the gas flow, computations were made by the method used by the manufacturer and the following equation was used:

$$W_g = C p_7 A_7 \sqrt{\frac{2\gamma g}{(\gamma - 1)R}} \sqrt{\frac{\left[\left(\frac{p_7}{p_7}\right)^{\frac{\gamma-1}{\gamma}} - 1\right] + \alpha\left[\left(\frac{p_7}{p_7}\right)^{\frac{\gamma-1}{\gamma}} - 1\right]^2}{T_{i,7}}}$$

The values of γ and R used in this equation were assumed constant and equal to 1.33 and 53.4, respectively; the same values were used by the manufacturer. The calibration constant C was also developed by the manufacturer to correct the calculated gas flows to actual values. This constant therefore served as a correction for systematic errors in measurement at station 7, for the expansion of the

tail pipe at station 7 with temperature, and for the error introduced into the calculations by the assumption of a constant value of γ.

The air flow was obtained from

$$W_a = W_g - W_f$$

The air flow through each combustion chamber W was considered to be one-fourteenth of the total air flow.

Combustion efficiency. - The combustion efficiency is defined as the ratio of the actual increase in enthalpy of the gas across the combustion chamber to the theoretical increase that would result from complete combustion of the fuel charge. The lower heating value of the fuel used was 18,600 Btu per pound; the following expression was therefore used in the computations:

$$\eta_b = \frac{c_{p,b}\,(T_5 - T_4)(1 + W_a/W_f)}{18,600}$$

Pressure losses. - The calculated pressure losses for the type C combustion chamber were obtained by means of the pressure-loss chart shown in figure 3. A similar chart was used to obtain comparable data for the type E combustion chamber. The development and use of this type of pressure-loss chart are explained in reference 5. The lines in quadrants I and IV, characteristic of the type C combustion chamber, were established from measured data in the manner described in reference 5. The term K represents the friction pressure-loss characteristics of the combustion chamber. Its significance is clarified by the following equation:

$$\frac{\Delta P_F}{P_4} = K \frac{W^2\,T_4}{P_4{}^2}$$

where ΔP_F is the pressure loss measured across the combustion chamber with the air flowing and no combustion (engine windmilling). The term A_B represents the cross-sectional area of an equivalent combustion chamber of uniform section having the same pressure losses due to heat addition to the air as in the actual combustion chamber. The lines in quadrant II were obtained by transferring the combustion-chamber-characteristic lines appearing in quadrant I to the second quadrant. This transfer was accomplished by using the

curves of constant M_4 appearing in quadrant II of the pressure-loss chart given in reference 5. The branching of the combustion-chamber-characteristic lines occurs at high combustion-chamber-inlet Mach numbers. After the characteristic lines were established, the pressure-loss chart was used in the following manner:

The value of the friction pressure-loss ratio $\Delta P_F/P_4$ was obtained on the ordinate in quadrant I by starting in quadrant IV with any given value of $W\sqrt{T_4/P_4}$ and proceeding counterclockwise. The value of the momentum pressure-loss ratio $\Delta P_M/P_B$ corresponding to the measured value of T_5/T_4 was found by proceeding through quadrant II and into quadrant III. The over-all pressure-loss ratio $\Delta P_T/P_4$ was then obtained from the relation

$$\Delta P_T = \Delta P_F + \Delta P_M$$

or

$$\frac{\Delta P_T}{P_4} = \frac{\Delta P_F}{P_4} + \frac{\Delta P_M}{P_4} \approx \frac{\Delta P_F}{P_4} + \frac{\Delta P_M}{P_B}$$

The value of K for the type C combustion chamber was determined from windmilling data. The value of K for the type E combustion chamber and the values of A_B for both types of combustion chamber were obtained from the charts by applying to actual experimental data the methods described in reference 5.

Cycle efficiency. - The cycle efficiency is defined by

$$\eta = \frac{\text{heat supplied by source - heat rejected to sink}}{\text{heat supplied by source}}$$

Expressed in terms of the quantities obtained from the instrumentation used, the efficiency is given by

$$\eta = \frac{c_{p,b}(T_5 - T_4) - c_{p,j}(t_9 - t_0)}{c_{p,b}(T_5 - T_4)}$$

The loss in cycle efficiency resulting from the pressure losses in the combustion chamber was calculated by the method given in reference 6:

$$\Delta\eta = \frac{c_{p,j}\, t_9 \left[1 - \left(\frac{P_5}{P_4} \right)^{\frac{\gamma-1}{\gamma}} \right]}{c_{p,b}\, (T_5 - T_4)}$$

Correlation of data for types C and E combustion chambers. - Average values of the pressures and temperatures over the entire tail-pipe cross-sectional area could be determined only from measurements obtained at station 8. Calculations for the type E combustion chamber, however, were necessarily based on measurements at station 7 inasmuch as no measurements were obtained at station 8 during tests with this combustion chamber. Owing to differences in instrumentation at these two stations, to probable errors in measurement caused by the proximity of station 7 to the turbine, and to heat losses between the stations (which is of least significance), data calculated from measurements at both stations could not be directly compared with satisfactory precision. Correlations were therefore developed with data from tests for which both measurements were available. Data presented for the type E combustion chamber were obtained by use of these correlations and are comparable to data presented for type C.

RESULTS AND DISCUSSION

Combustion Efficiency

The results presented cover the operable range of engine speeds at simulated altitudes from 10,000 to 50,000 feet from static conditions to a ram pressure ratio of 1.76.

Effect of engine speed and altitude. - The effect on combustion efficiency of variations in corrected engine speed and simulated altitude at a ram pressure ratio of approximately 1.10 is shown in figure 4 for the types C and E combustion chambers. The combustion efficiency decreases rapidly with decreasing engine speed. The rate of decrease with decreasing engine speed is generally greater for the type E combustion chamber than for type C. Maximum combustion efficiencies of 97 and 96 percent were obtained for the types C and E combustion chambers, respectively. This maximum value occurred near the rated engine speed.

At the highest corrected engine speeds, variations in simulated altitude from 10,000 to 30,000 feet have little effect on the combustion efficiency for either type of combustion chamber. At low engine speeds the combustion efficiency drops off rapidly with increasing altitude for both types of combustion chamber. Between 30,000 and 40,000 feet the combustion efficiency for the type E combustion chamber decreases approximately 20 to 35 percent in value over the range of engine speeds and a further decrease of about 20 percent occurs between 40,000 and 50,000 feet. The rate of decrease in efficiency is larger, in general, as the altitude increases. At a given altitude and corrected engine speed, the type C combustion chamber generally gives a higher combustion efficiency than type E.

One factor that may have contributed to the low combustion efficiency at low engine speeds and high altitudes is the probability of changed fuel-spray characteristics due to low fuel flows. With the standard Monarch fuel nozzles, higher fuel flows were required to keep the engine operating at low speeds than were required with duplex fuel nozzles, which were briefly investigated during the program. Each of the duplex nozzles contained two fuel-discharge orifices. The small orifice alone discharged fuel at low fuel flows; whereas for high fuel flows both orifices operated. The maximum fuel-discharge rate for the duplex nozzles was 45 gallons per hour. With this arrangement more uniform fuel-spray characteristics and better atomization of the fuel were obtainable at low fuel flows than were obtainable with a nozzle having a single fuel-discharge orifice capable of giving the high fuel flows required for operation at the engine speeds encountered in flight.

The following table gives values of the fuel flow at an engine speed of 4500 rpm for the engine equipped with standard Monarch fuel nozzles and using kerosene as fuel and equipped with duplex nozzles and using kerosene and gasoline as fuels:

Nozzle	Fuel	Fuel flow (lb/hr)
Monarch, 40 gal/hr	Kerosene	640
Duplex, 45 gal/hr	Kerosene	440
Duplex, 45 gal/hr	Gasoline	380

These values are averages for comparable ram pressure ratios and altitudes and were obtained while all combustion chambers were operating. The greater fuel flow when the engine was equipped with

Monarch nozzles indicates that a lower combustion efficiency was obtained with this type of nozzle at low engine speeds than was obtained when the duplex nozzles were used. The tabulated fuel-flow values indicate that higher combustion efficiencies were obtained when the duplex nozzles were used with gasoline than when they were used with kerosene, for both fuels have approximately the same heating value. This difference indicates that further development of fuel nozzles should result in an improvement of combustion efficiency (and a consequent decrease in fuel flow) at low engine speeds when kerosene is used as the fuel.

Effect of ram pressure ratio. - The combustion efficiency increases with ram pressure ratio at a constant simulated altitude and corrected engine speed (fig. 5). The efficiency increases from 94 to 97 percent at a corrected engine speed of 12,000 rpm and from 84 to 90 percent at 10,000 rpm with a change from static conditions (ram pressure ratio, 0.98) to a ram pressure ratio of 1.76 at an altitude of 30,000 feet. The occurrence of a ram pressure ratio smaller than 1.0 for static conditions is caused by the loss in total pressure in the inlet ducts, which gives a total pressure at the compressor inlet lower than the tunnel static pressure.

Correlation of combustion efficiency with combustion-chamber operating variables. - Reference 7 showed that combustion efficiency in an annular combustion chamber was increased as combustion-chamber-inlet pressure and temperature were increased and was decreased as inlet-air velocity was increased. The trends in combustion efficiency with these parameters are probably also applicable in the I-40 engine. For the data presented, an increase in simulated altitude for constant corrected engine speed and ram pressure ratio results in lower combustion-chamber-inlet pressures and temperatures and higher combustion-chamber-inlet velocities. According to reference 7, all these changes would result in the observed lowering of combustion efficiencies with increasing altitude. When the ram pressure ratio is increased at constant altitude and corrected engine speed, each of the three parameters increases. An increase in combustion-chamber-inlet temperature and pressure tends to give an increased combustion efficiency; whereas a higher combustion-chamber-inlet velocity results in a lower efficiency. These results could explain the moderate increase in combustion efficiency with increasing ram pressure ratio.

A method of correlating the combustion efficiency with the combustion-chamber-outlet temperature was presented in reference 6. In this correlation the product of the combustion efficiency and the square root of the combustion-chamber-outlet temperature

$\eta_b \sqrt{T_5}$ is plotted on a logarithmic scale against the reciprocal of the combustion-chamber-outlet temperature $1/T_5$ for constant values of the parameter, combustion-chamber-inlet pressure divided by the square of the air flow P_4/W^2. Figure 6 shows such a correlation for the type C combustion chamber for two ranges of the parameter. The points shown are actual data points covering the complete range of ram pressure ratios, altitudes, and engine speeds discussed. Ranges of the parameter rather than single fixed values are shown in order that sufficient data points might be available to define the curves. Straight lines are established by the data for both ranges of the parameter given. This correlation is a semiempirical relation and, although applicable to the present data as well as to those of reference 6, should not be considered generally established.

Combustion-Chamber Pressure Losses

Losses in total pressure occurring during the passage of the gas through the combustion chamber are shown in figures 7 and 8. The losses are given as the ratio of the pressure loss to the combustion-chamber-inlet total pressure. The over-all pressure loss can be considered as the sum of two separate losses: one due to the friction of the flow and the other due to the addition of heat to the flowing air (reference 5). By means of the pressure-loss chart (fig. 3), the over-all pressure loss was separated into these component parts; the ratios of each to the combustion-chamber-inlet total pressure are also plotted in these figures.

Effect of engine speed and altitude. - The measured values of the over-all pressure-loss ratio are in agreement with the values calculated by use of the pressure-loss chart for both the type C and type E combustion chambers at simulated altitudes as high as 30,000 feet (fig. 7). These data are for a ram pressure ratio of approximately 1.10. At altitudes of 40,000 and 50,000 feet, the measured values of the over-all pressure-loss ratio for the type E combustion chamber are larger than the calculated values. This difference between experimental data and computed values may be caused by inaccuracies in measuring the pressures. At the high altitudes, a given increment of error in measurement would represent a larger proportion of the pressure measured than at low altitudes.

For the type C combustion chamber, the over-all pressure-loss ratio maintains a value of about 0.06 over most of the operating range. The lowest values of the over-all pressure-loss ratio

(about 0.04) occur at the lowest corrected engine speeds, and peak values are obtained at intermediate speeds. The pressure losses for the type E combustion chamber are in general slightly smaller than for the type C combustion chamber and tend to decrease more in the high engine-speed range. Changes in altitude have negligible effect on the over-all pressure-loss ratio.

Neither the friction pressure-loss ratio nor the momentum pressure-loss ratio for the type C combustion chamber is significantly affected by changes in altitude. At the highest corrected engine speeds these two pressure losses are approximately equal. At lower speeds the pressure loss due to friction is greater than that due to the addition of heat. At simulated altitudes up to 30,000 feet, the friction pressure-loss ratios for the types E and C combustion chamber are approximately equal; whereas the momentum pressure-loss ratio is lower for type E than for type C. The differences between measured and calculated over-all pressure-loss ratios for the type E combustion chamber at altitudes of 40,000 and 50,000 feet probably make any precise comparison of the relative magnitudes of the two component pressure losses under these conditions unwarranted.

The relative magnitudes of the pressure losses for the different types of combustion chamber can be explained by reference to the equivalent areas A_B and the friction pressure-loss factors K for the two types. These values for a single combustion chamber are as follows:

Combustion-chamber type	A_B (sq ft)	K
C	0.126	1.47
E	.134	1.62

Because the momentum pressure loss varies inversely with A_B and the friction pressure loss varies directly with K, the occurrence of higher values for both factors with the type E combustion chamber produced counteracting changes that resulted in a slightly lower over-all pressure loss than was obtained with the type C combustion chamber.

Effect of ram pressure ratio. - The pressure-loss ratios for the type C combustion chamber at a simulated altitude of 30,000 feet and over a range of ram pressure ratios from 0.98 (static conditions) to 1.76 are shown in figure 8. The calculated and measured over-all pressure-loss ratios are in agreement for all ram pressure ratios up to 1.26. Changes of ram pressure ratio within this range have little

effect on the over-all pressure-loss ratio. The friction and momentum pressure losses are about equal for static conditions over the entire engine-speed range. At values of the corrected engine speed near 12,000 rpm, increasing the ram pressure ratio has slight effect on either the friction or momentum pressure-loss ratios. At lower corrected engine speeds, however, the friction pressure-loss ratio increases and the momentum pressure-loss ratio decreases slightly with increasing ram pressure ratio.

The measured values of the over-all pressure-loss ratio are consistently higher than the calculated values at ram pressure ratios of 1.53 and 1.76. This discrepancy can be explained by reference to figure 9, where the combustion-chamber-inlet Mach number is plotted against the corrected engine speed for three different ram pressure ratios at a simulated altitude of 30,000 feet. At a constant corrected engine speed the combustion-chamber-inlet Mach number increases with an increase in ram pressure ratio. At the high inlet Mach numbers, the location of the origin of the flame may have changed or the gas flow may have streamed through the combustion chambers in such a manner that only part of the cross-sectional area of the combustion liner was utilized for combustion. If either of these phenomena occurred, a lower equivalent area and, consequently, a higher momentum pressure loss than at low Mach numbers would result. The data for these conditions indicated that a smaller value for the equivalent combustion-chamber area was applicable during operation at high ram pressure ratios than at low ram pressure ratios. In the pressure-loss chart (fig. 3) the lines marked "A_B constant" were established by the data for low ram pressure ratios and were used in calculating the pressure losses for all conditions under which the standard combustion chamber was tested. The lines marked "A_B varying" were determined by some of the data for the higher ram pressure ratios and combustion-chamber-inlet Mach numbers. Duplicate calculations using these "A_B varying" lines were made for the data obtained at ram pressure ratios of 1.53 and 1.76. Two curves are thus given for the momentum pressure-loss ratio (and consequently for the calculated over-all pressure-loss ratio) for these two operating conditions in figure 8. In general, the measured pressure losses lie between the curves calculated from the two sets of characteristic lines of figure 3. This phenomenon is interpreted to mean that the average effective cross-sectional area of the 14 individual combustion chambers changed gradually and that this area was generally larger than the equivalent combustion-chamber area used to obtain the "A_B varying" lines.

The characteristic lines of figure 3 representing a varying cross-sectional area were established by the portions of the experimental data of the complete program that deviated most from the predicted values. Consequently, any experimental data for the type C combustion chamber obtained within the operating range covered in this investigation will probably either be represented by calculations based on a constant equivalent area or be within the range established by the two sets of calculations.

Predicted pressure losses up to ram pressure ratios of about 1.3 are in agreement with the measured losses. The minimum flight velocity corresponding to this ram pressure ratio is 413 miles per hour at altitudes greater than 37,000 feet. The ram pressure ratio of 1.76 corresponds to a flight velocity of 620 miles per hour at the same altitudes. Consequently, combustion-chamber pressure losses for the I-40 jet-propulsion engine can be accurately predicted by the method of reference 5 for flight velocities up to 400 miles per hour. Moderate errors are encountered when similar predictions are made for flight velocities from 400 to 600 miles per hour.

Losses in Engine-Cycle Efficiency Due to Combustion-Chamber Pressure Losses

Effect of variations in engine speed and altitude. - The fractional loss in engine-cycle efficiency due to combustion-chamber pressure losses $\Delta\eta/\eta$ for engine configurations having the types C and E combustion chambers is shown in figure 10 for a ram pressure ratio of approximately 1.10. At the rated engine speed of 11,500 rpm, corresponding to the highest corrected engine speed on each curve in figure 10, a minimum fractional loss in engine-cycle efficiency of about 0.08 is obtained with the configuration using the type C combustion chamber. A minimum value of about 0.05 is encountered with the engine configuration having the type E combustion chamber under the same conditions. The fractional loss increases rapidly as the engine speed is decreased, generally reaching a value of one-half at a corrected engine speed between 6000 and 8000 rpm. The effect of changes in simulated altitude at constant values of corrected engine speed is shown by the cross plots of figure 11. In general, a slight increase in engine-cycle-efficiency fractional losses due to combustion-chamber pressure losses is indicated with increasing altitude.

The lower fractional loss in engine-cycle efficiency for the type E combustion chamber as compared to that for the type C

chamber (fig. 10) is the result of the lower over-all pressure losses encountered with this combustion chamber (fig. 7), which are most noticeable at high engine speeds. The losses in engine-cycle efficiency at high engine speeds are so low as to have a negligible effect on the performance of the unit. The fractional losses at the lower engine speeds are larger and would be of importance in operation at low speeds or in acceleration of the engine from low speeds.

Effect of ram pressure ratio. - The effect on engine-cycle efficiency and on the fractional loss in engine-cycle efficiency due to combustion-chamber pressure losses of variations in ram pressure ratio at a simulated altitude of 30,000 feet is shown in figures 12 and 13 for the type C combustion chamber. The fractional losses in cycle efficiency due to combustion-chamber pressure losses decrease with an increase in ram pressure ratio.

SUMMARY OF RESULTS

An altitude-wind-tunnel investigation of the complete I-40 jet-propulsion engine gave the following results on the operating characteristics of the combustion chambers:

1. Maximum combustion efficiencies of 97 and 96 percent were obtained with the types C and E combustion chambers, respectively, at a ram pressure ratio of approximately 1.10. At comparable operating conditions the type C combustion chamber gave generally higher combustion efficiency than did the type E.

2. Combustion efficiency varied directly with the engine speed and ram pressure ratio. The combustion efficiency decreased with increasing altitude; at low engine speeds the decrease was greater than at high speeds.

3. Combustion efficiency could be correlated with the combustion-chamber-outlet temperature. When the product of the combustion efficiency and the square root of the combustion-chamber-outlet temperature was plotted on a logarithmic scale against the reciprocal of the same temperature, straight lines were established for constant values of the parameter, combustion-chamber-inlet pressure divided by the square of the air weight flow.

4. Combustion-chamber pressure losses of about 6 percent of the combustion-chamber-inlet total pressure were obtained with the type C

combustion chamber over most of the operating range. Slightly lower pressure losses were obtained with the type E combustion chamber.

5. Percentage losses in combustion-chamber total pressure were negligibly affected by changes in altitude or in ram pressure ratio up to approximately 1.3.

6. A pressure-loss chart could be used to predict with fair accuracy the pressure-loss characteristics of these combustion chambers under most flight conditions.

7. At rated engine speed and a ram pressure ratio of approximately 1.10, losses in total pressure in the combustion chambers caused fractional losses in engine-cycle efficiency of about 0.08 and 0.05 for the types C and E combustion chambers, respectively. The fractional losses varied inversely as the engine speed, generally reaching a value of one-half at a corrected engine speed between 6000 and 8000 rpm.

Flight Propulsion Research Laboratory,
National Advisory Committee for Aeronautics,
Cleveland, Ohio.

REFERENCES

1. Gendler, Stanley L., and Koffel, William K.: Investigation of the I-40 Jet-Propulsion Engine in the Cleveland Altitude Wind Tunnel. I - Performance and Windmilling Drag Characteristics. NACA RM No. E8G02, 1948.

2. Dietz, Robert O., Jr., and Geisenheyner, Robert M.: Investigation of the I-40 Jet-Propulsion Engine in the Cleveland Altitude Wind Tunnel. II - Analysis of the Compressor Performance Characteristics. NACA RM No. E8G02a, 1948.

3. Krebs, Richard P., and Foshag, Frederick C.: Investigation of the I-40 Jet-Propulsion Engine in the Cleveland Altitude Wind Tunnel. III - Analysis of Turbine Performance and Effect of Tail-Pipe Design on Engine Performance. NACA RM No. E8G02b, 1948.

4. Turner, L. Richard, and Lord, Albert M.: Thermodynamic Charts for the Computation of Combustion and Mixture Temperatures at Constant Pressure. NACA TN No. 1086, 1946.

5. Pinkel, I. Irving, and Shames, Harold: Analysis of Jet-Propulsion Engine Combustion-Chamber Pressure Losses. NACA TN No. 1180, 1947.

6. Pinkel, I. Irving, and Shames, Harold: Altitude-Wind-Tunnel Investigation of a 4000-Pound-Thrust Axial-Flow Turbojet Engine. VI - Combustion-Chamber Performance. NACA RM No. E8F09e, 1948.

7 Childs, J. Howard, McCafferty, Richard J., and Surine, Oakley W.: Effect of Combustor-Inlet Conditions on Performance of an Annular Turbojet Combustor. NACA TN No. 1357, 1947.

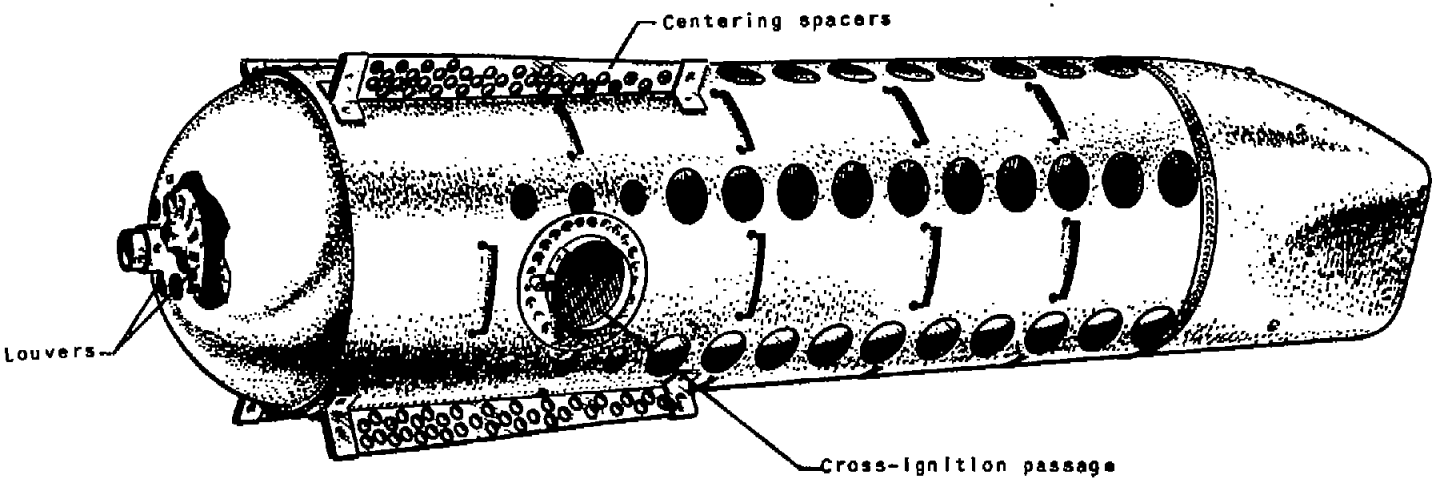

Type C liner and dome

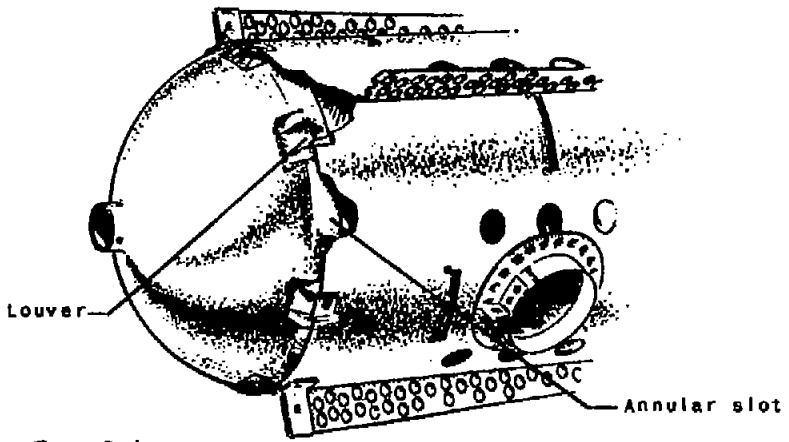

Type E dome

Figure 1. - Combustion-chamber liners used in I-40 jet-propulsion engine.

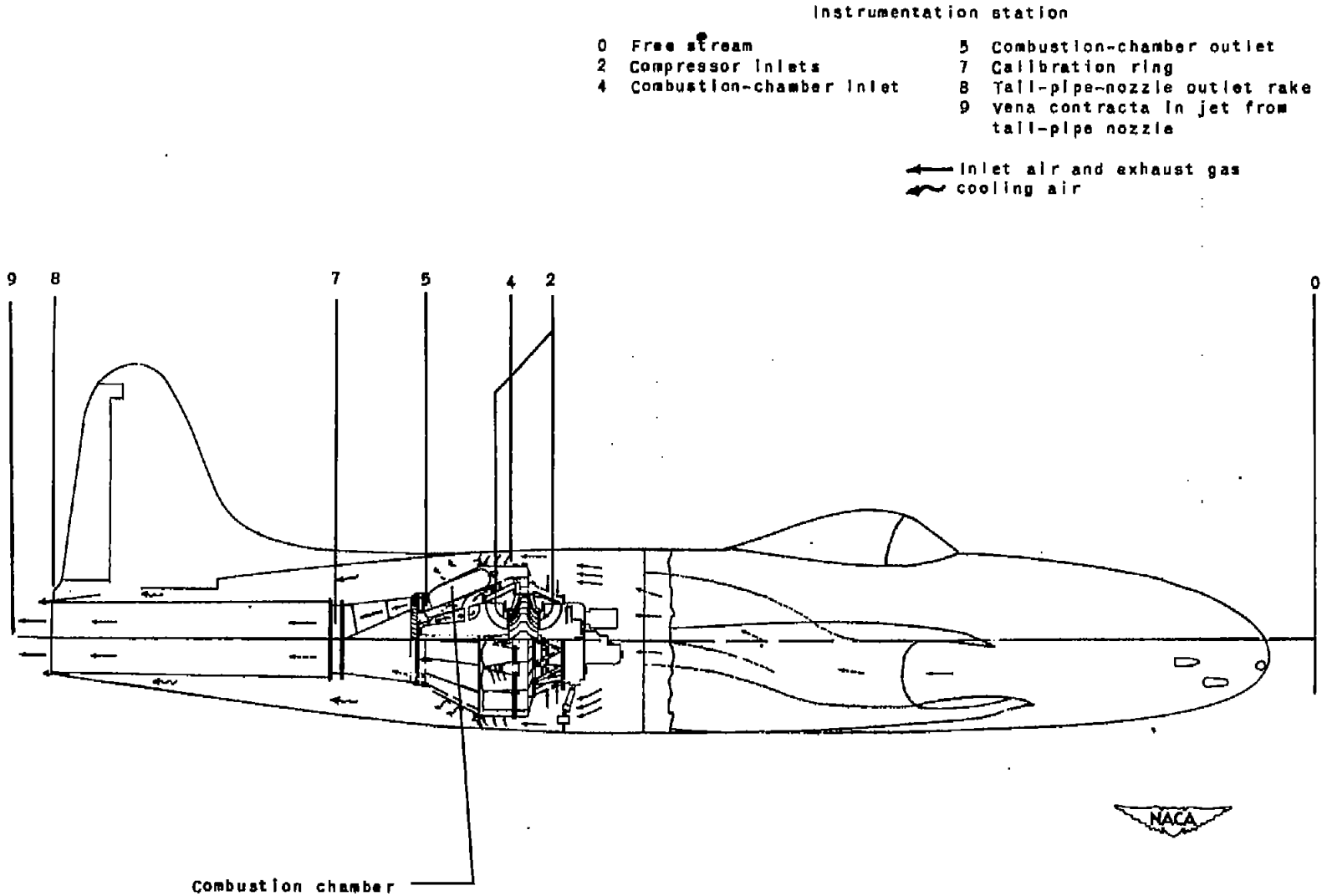

Figure 2. -- I-40 jet-propulsion engine installed in airplane fuselage.

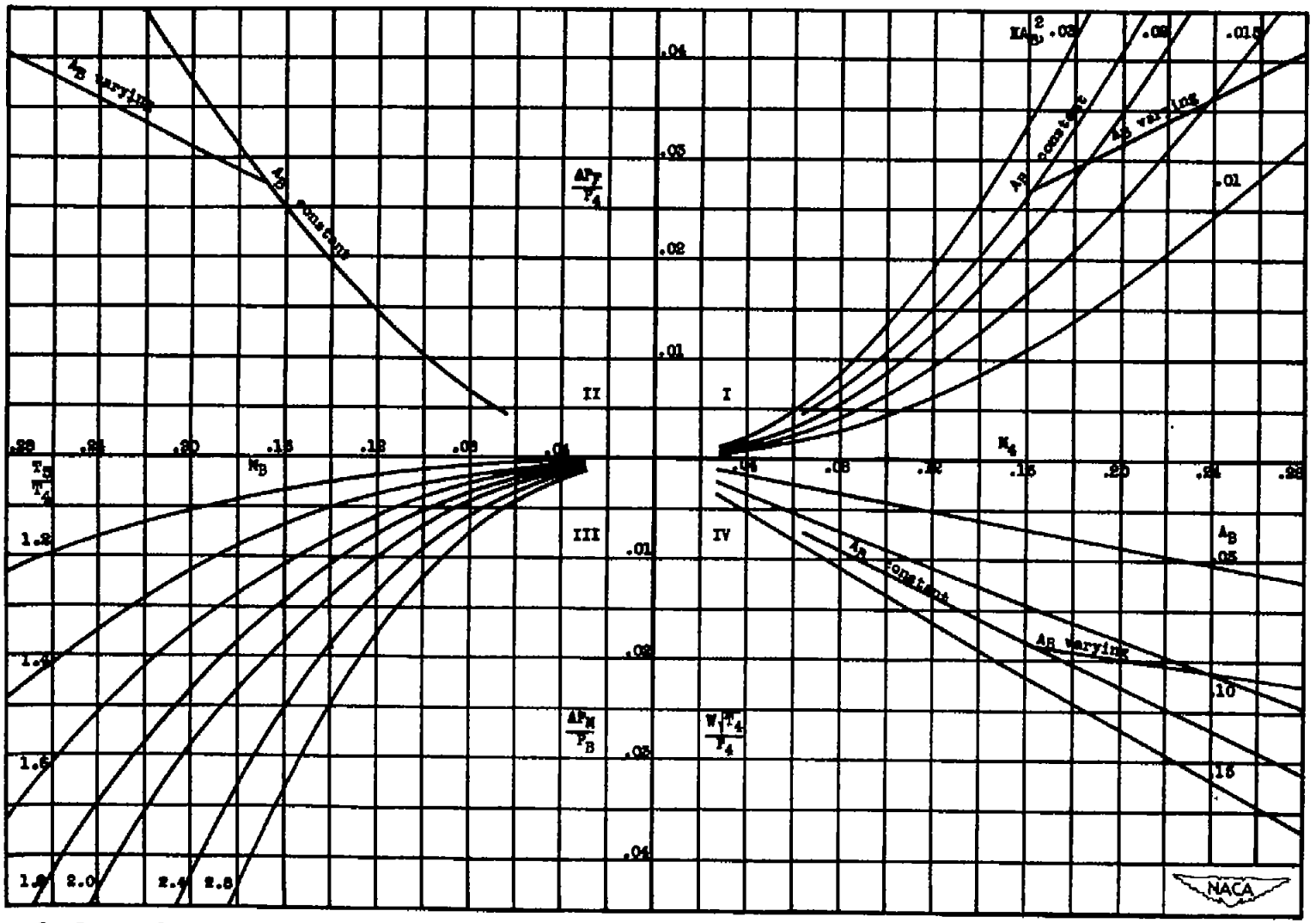

Figure 3.- Pressure-loss chart used to calculate losses in total pressure for type C combustion chamber.

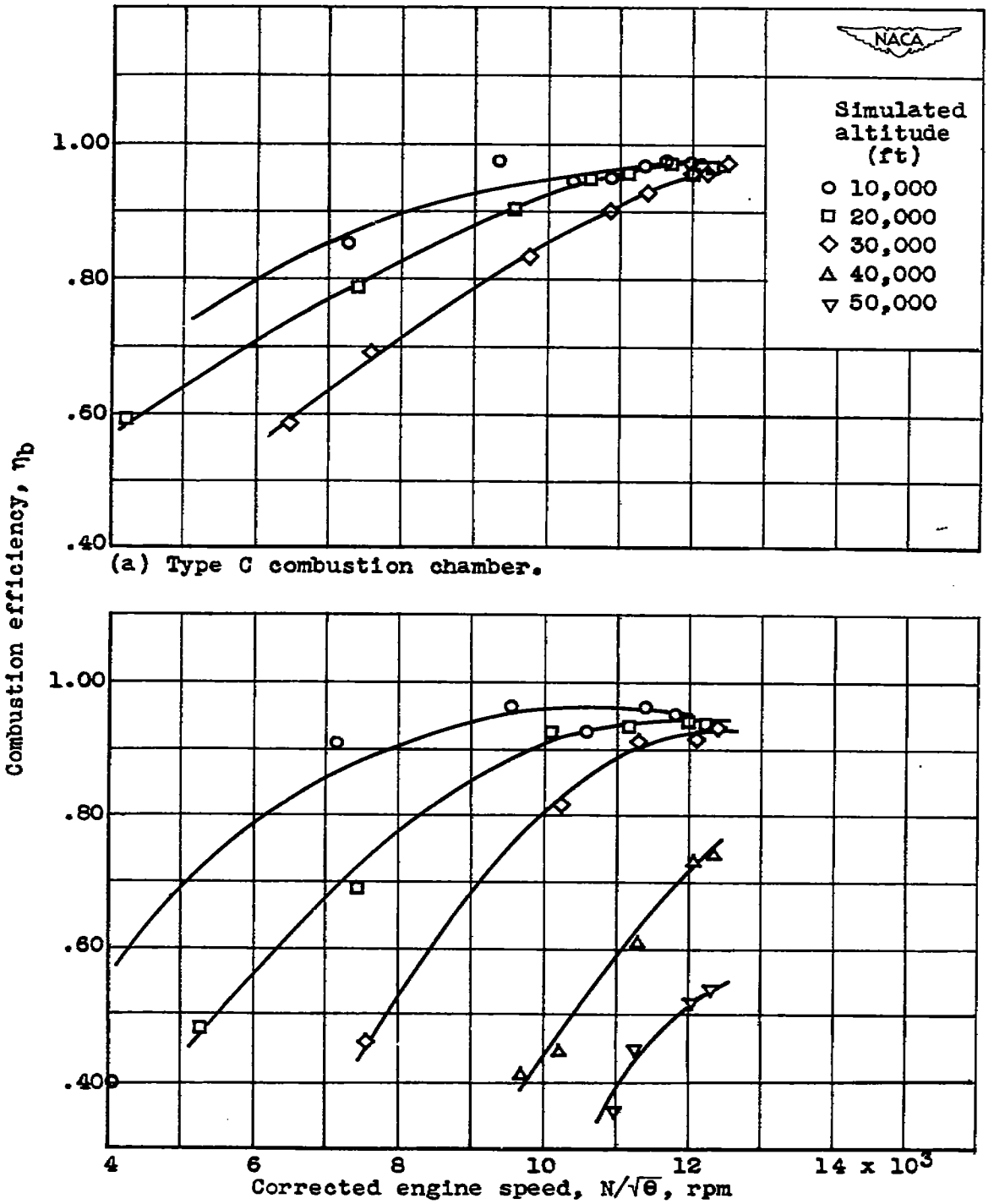

(a) Type C combustion chamber.

(b) Type E combustion chamber.

Figure 4.- Effect on combustion efficiency of variations in corrected engine speed and simulated altitude at ram pressure ratio of approximately 1.10.

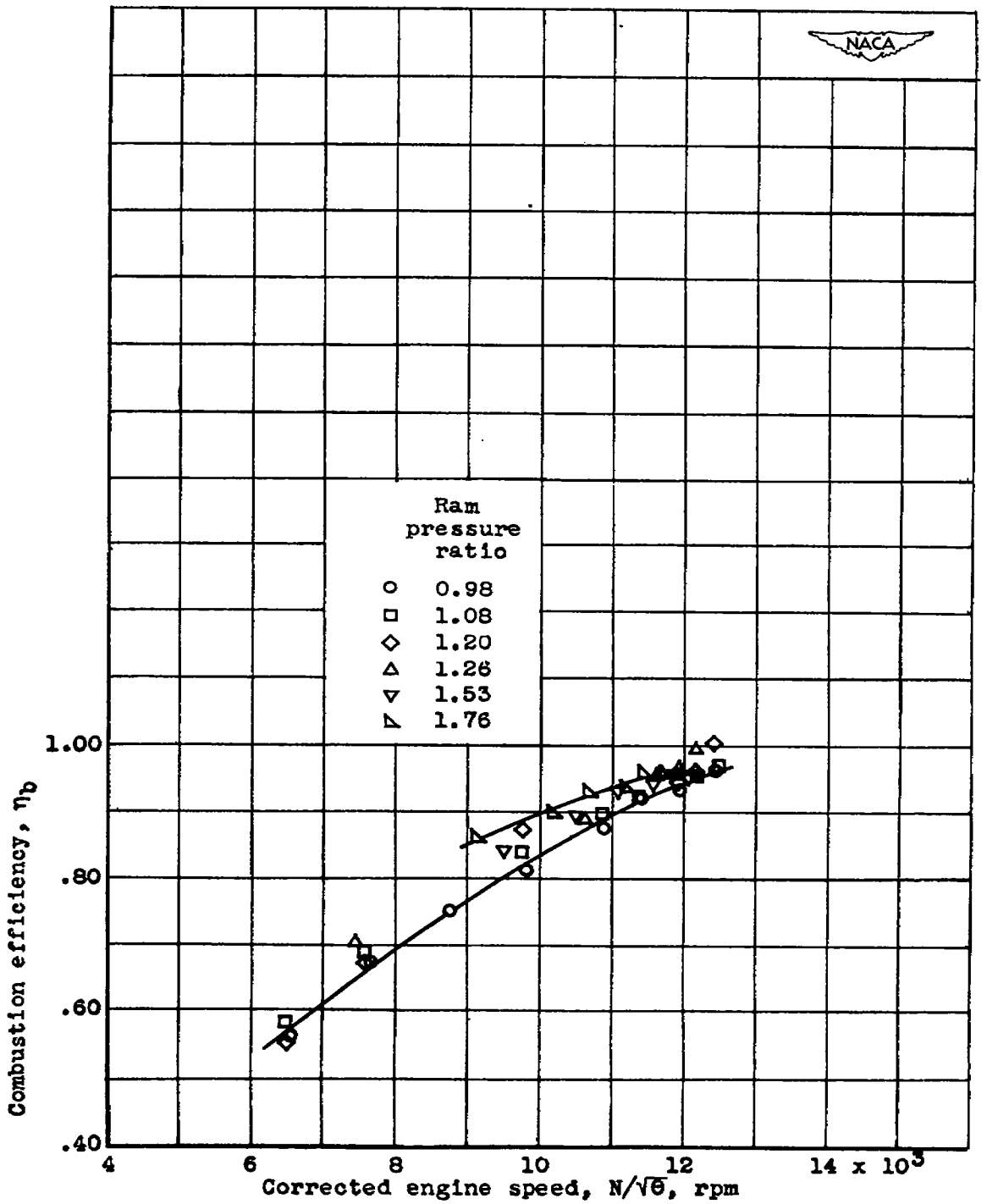

Figure 5.- Effect on combustion efficiency for type C combustion chamber of variations in corrected engine speed and ram pressure ratio at simulated altitude of 30,000 feet.

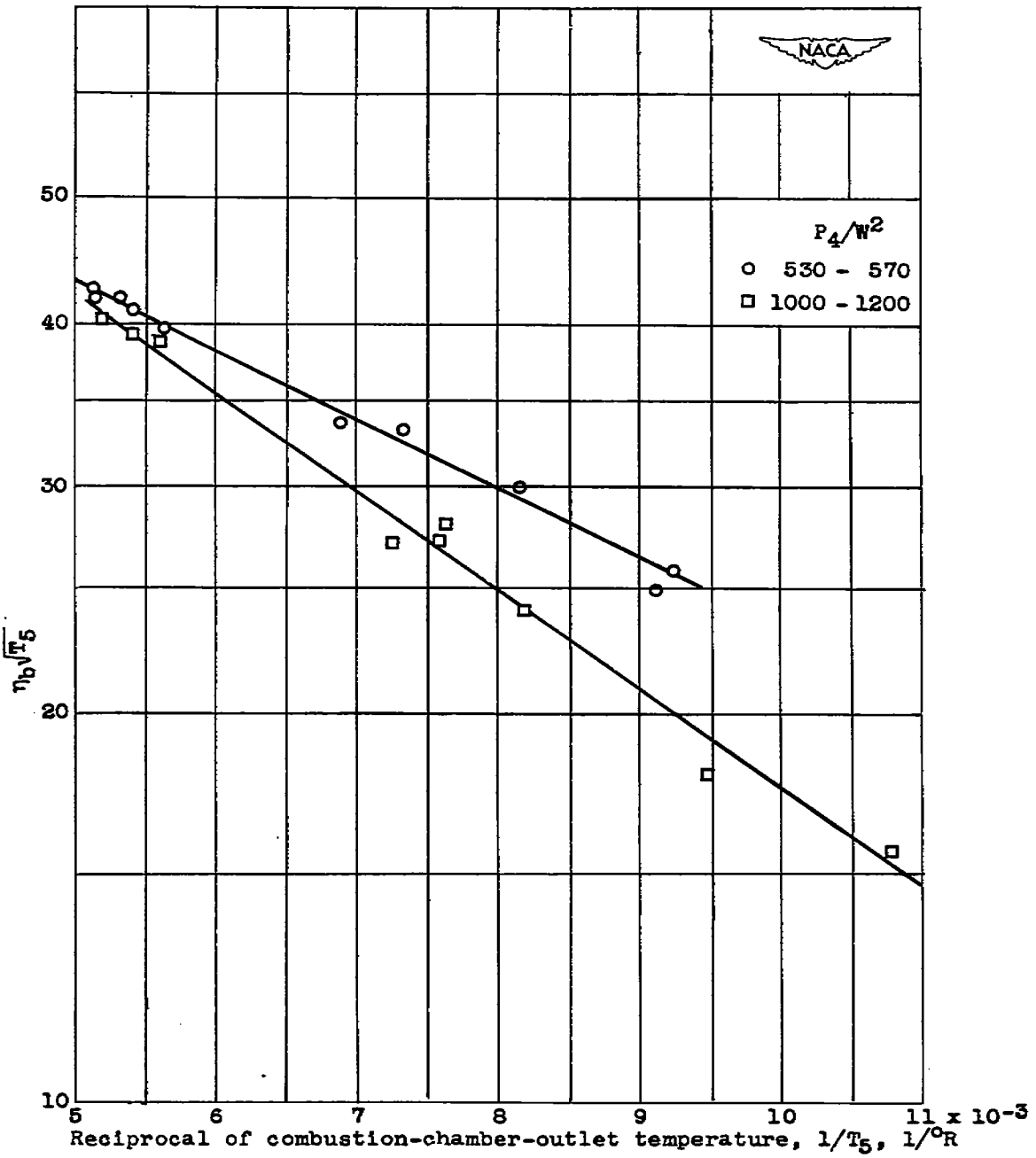

Figure 6.- Correlation of combustion efficiency with combustion-chamber-outlet temperature for type C combustion chamber. Ram pressure ratio, 0.98 to 1.76; engine speed, 5000 to 12,000 rpm; simulated altitude, 10,000 to 50,000 feet.

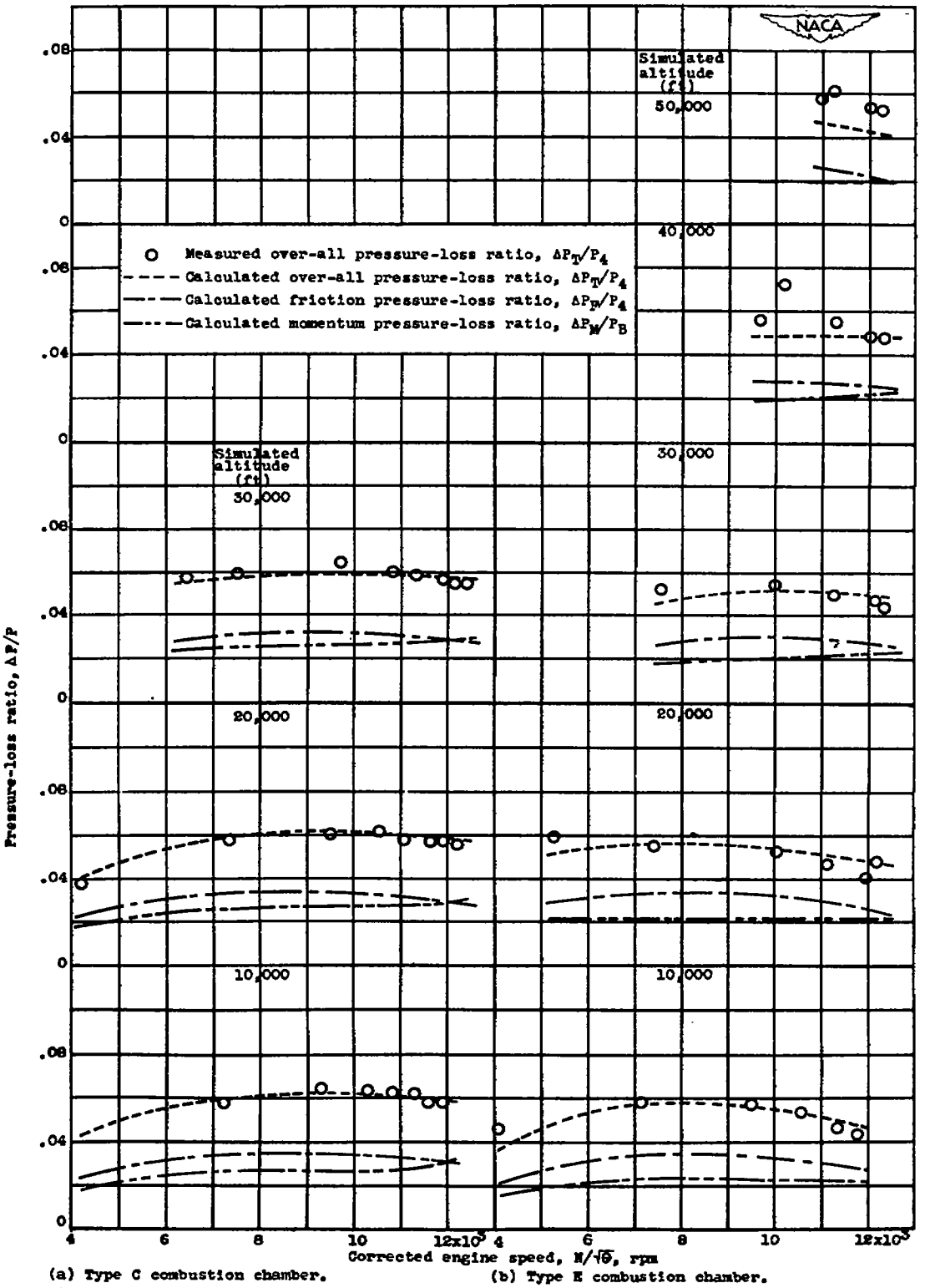

(a) Type C combustion chamber. (b) Type E combustion chamber.

Figure 7.- Comparison of pressure losses for types C and E combustion chambers for various simulated altitudes at ram pressure ratio of approximately 1.10.

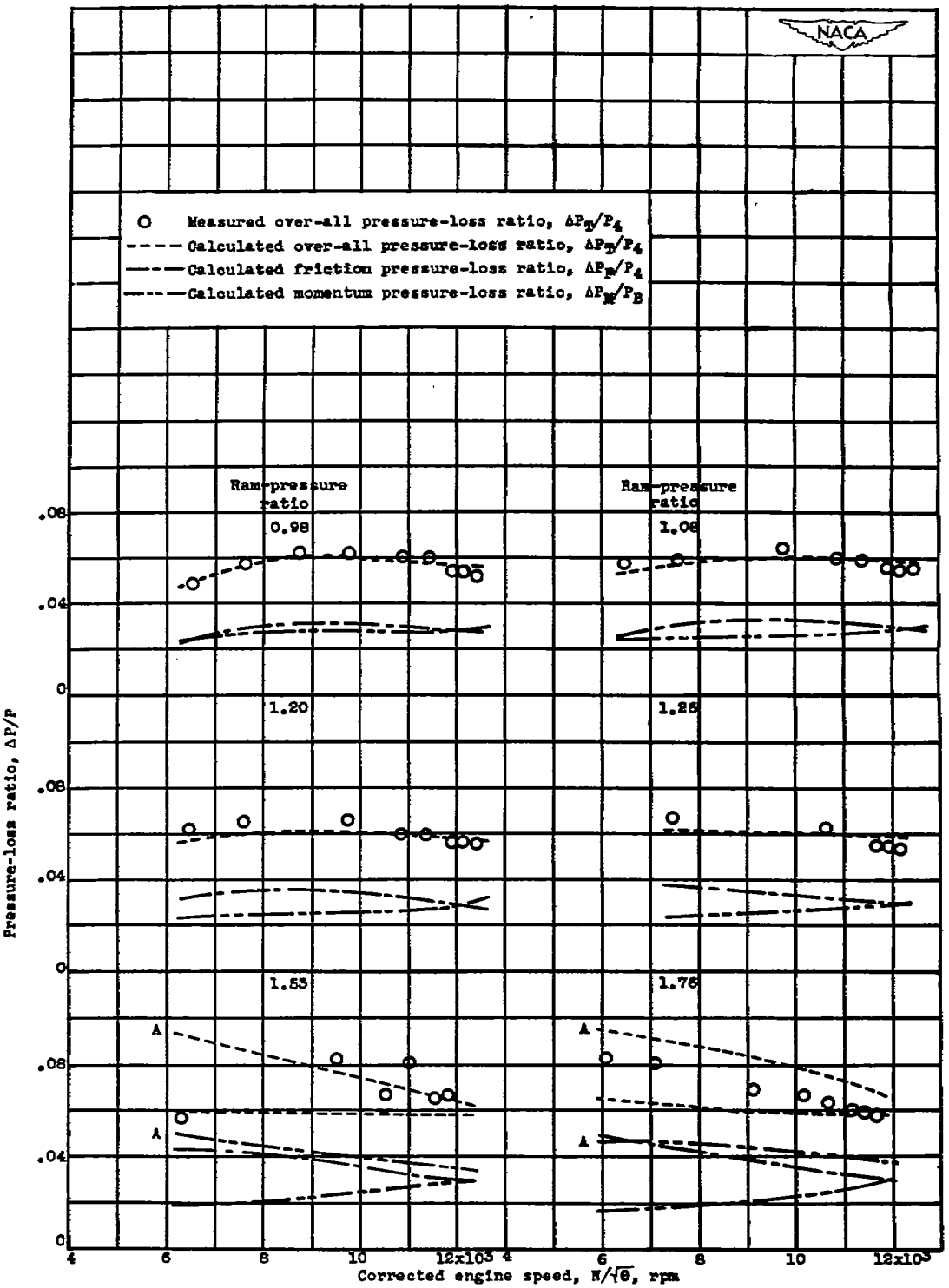

Figure 8.- Effect of ram pressure ratio on pressure losses for type C combustion chamber at simulated altitude of 30,000 feet. Curves A are values calculated with assumption of lowered effective combustion-chamber cross-sectional area at high values of combustion-chamber-inlet Mach number.

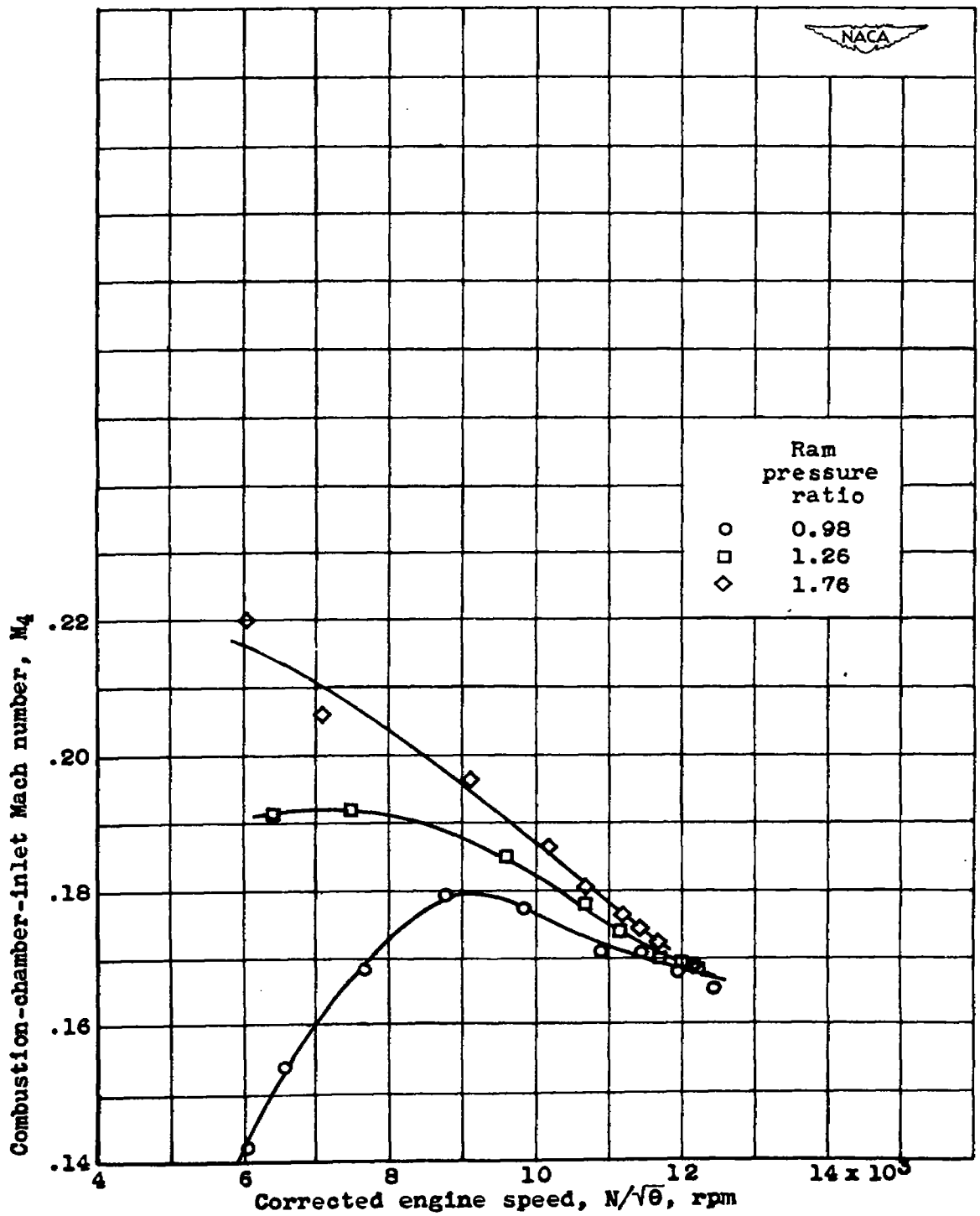

Figure 9.- Variation of combustion-chamber-inlet Mach number with ram pressure ratio and corrected engine speed for type C combustion chamber at simulated altitude of 30,000 feet.

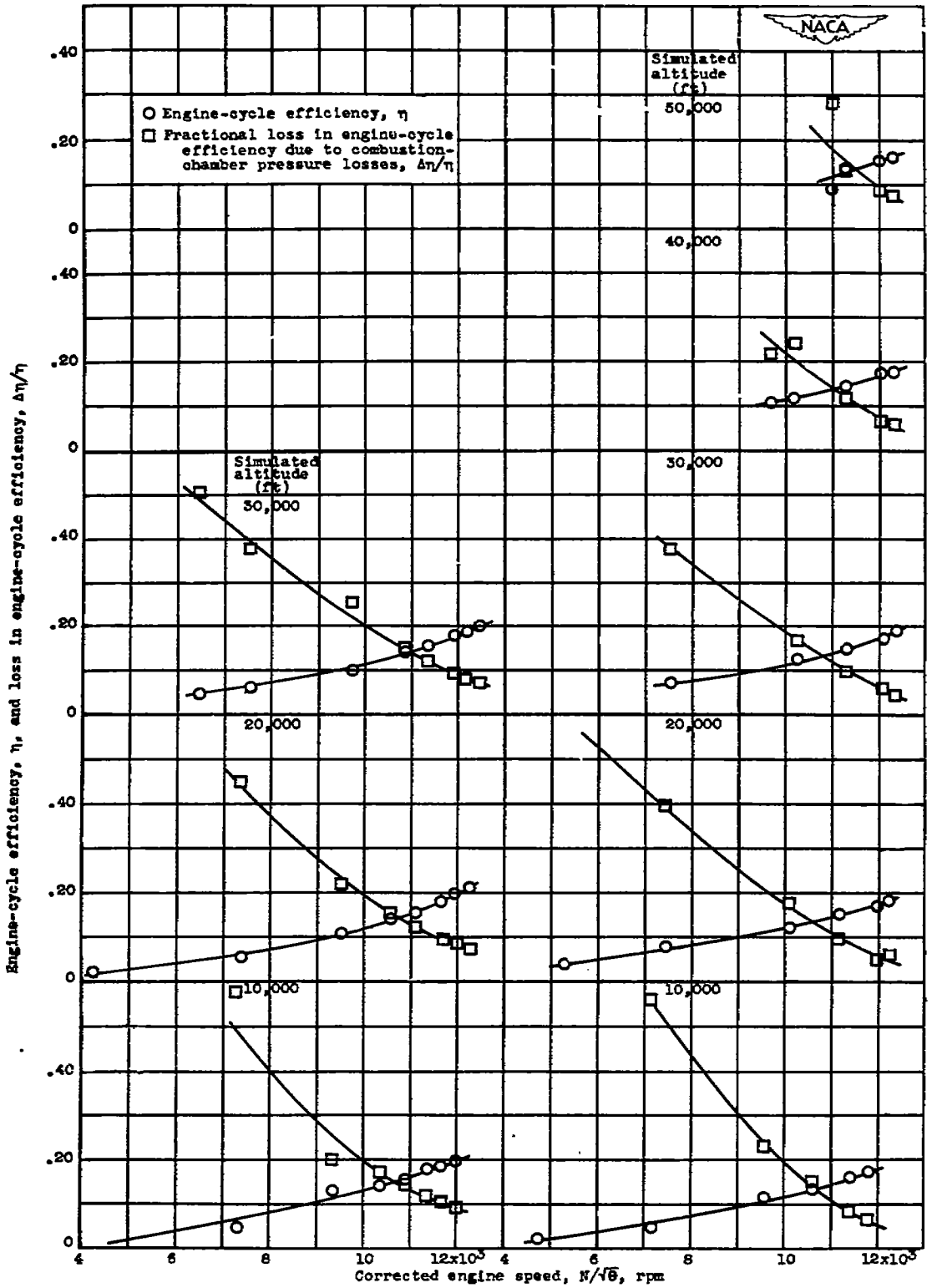

(a) Type C combustion chamber. (b) Type E combustion chamber.

Figure 10.- Comparison of engine-cycle efficiencies and fractional losses in engine-cycle efficiency due to combustion-chamber pressure losses for types C and E combustion chambers for various simulated altitudes at ram pressure ratio of approximately 1.10.

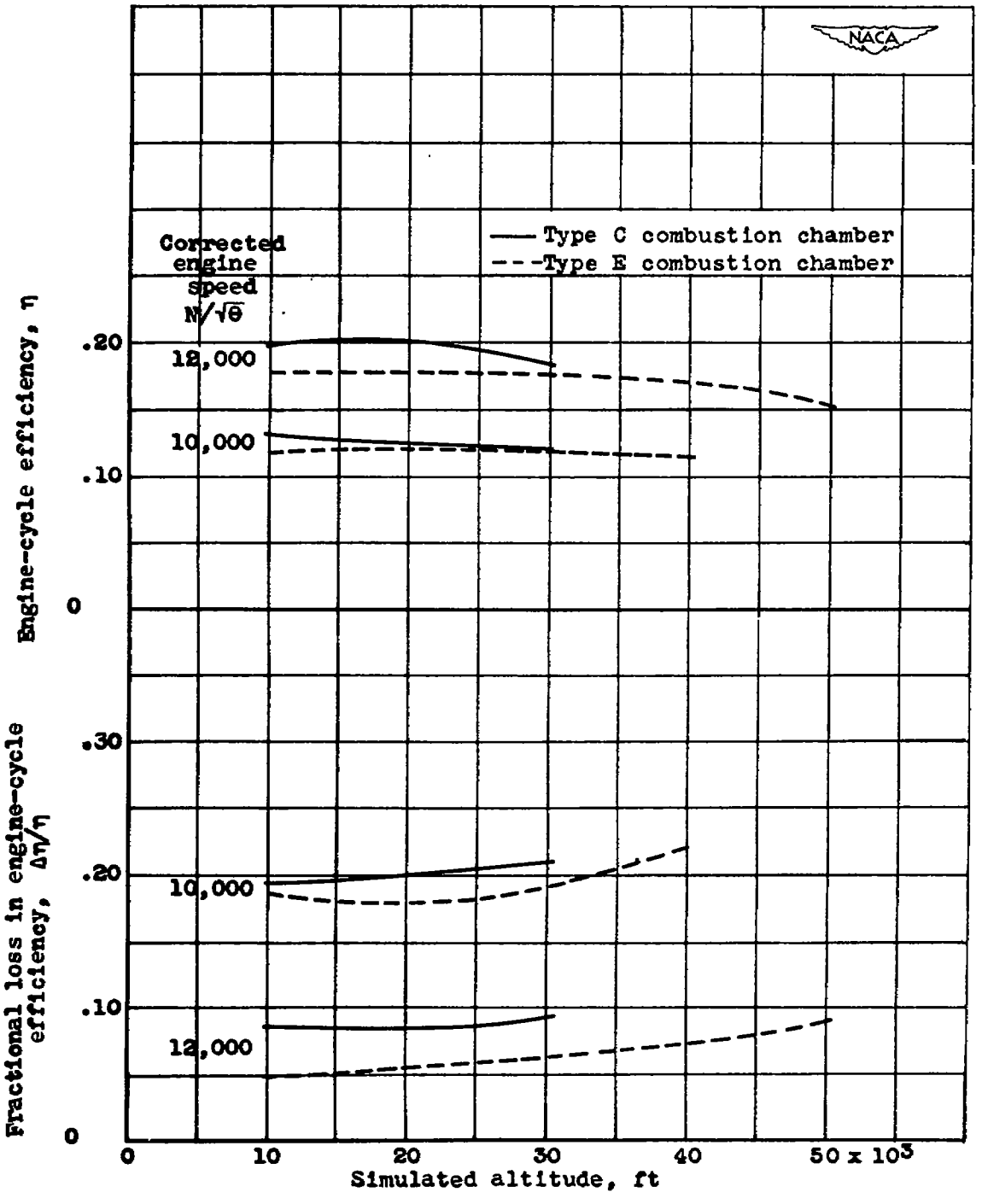

Figure 11.- Variation with altitude of engine-cycle efficiency and fractional loss in engine-cycle efficiency due to combustion-chamber pressure losses of types C and E combustion chambers for constant values of corrected engine speed at ram pressure ratio of approximately 1.10.

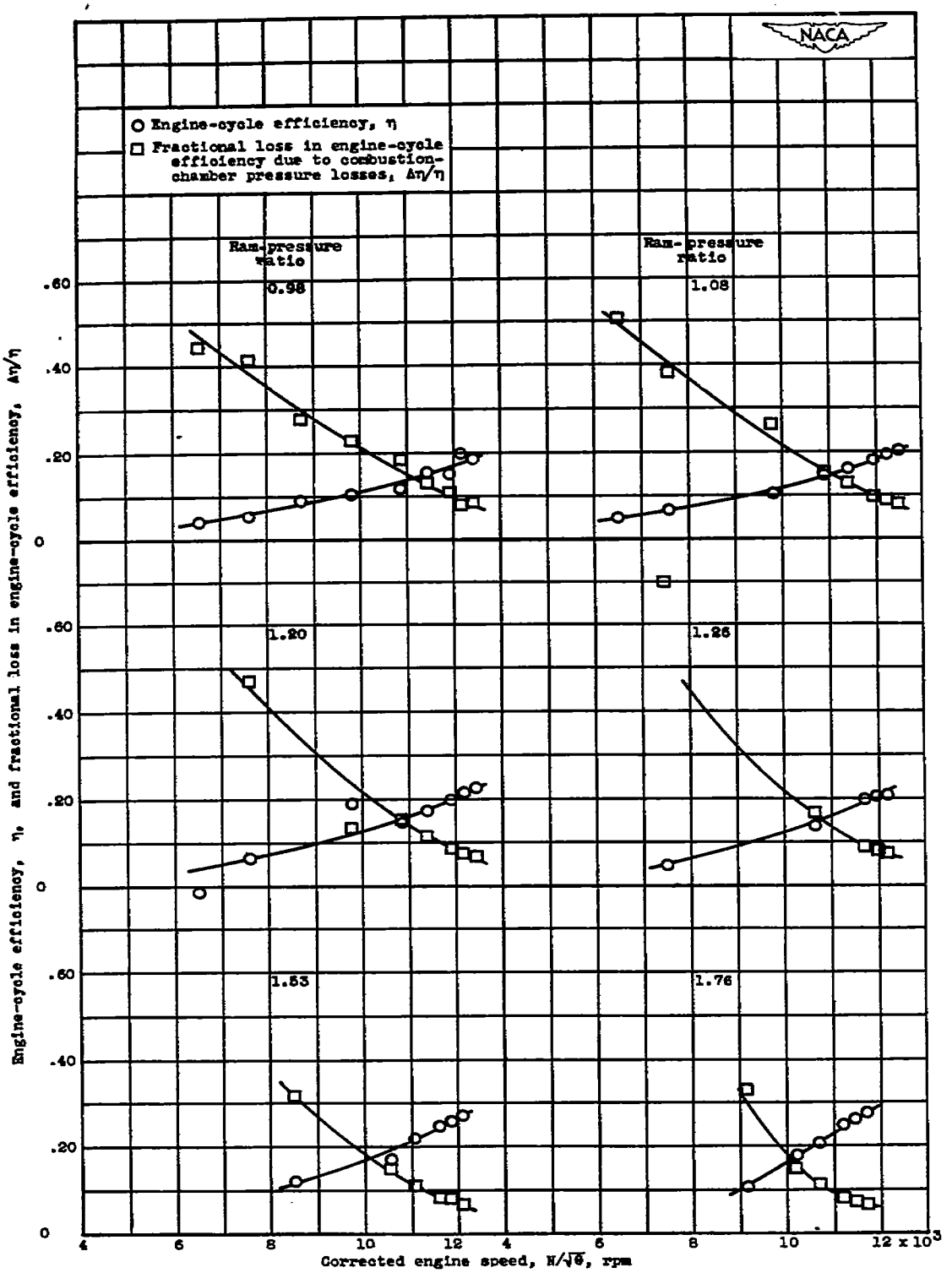

Figure 12.- Effect on engine-cycle efficiency and fractional loss in engine-cycle efficiency due to combustion-chamber pressure losses of variations in ram pressure ratio for type C combustion chamber at simulated altitude of 30,000 feet.

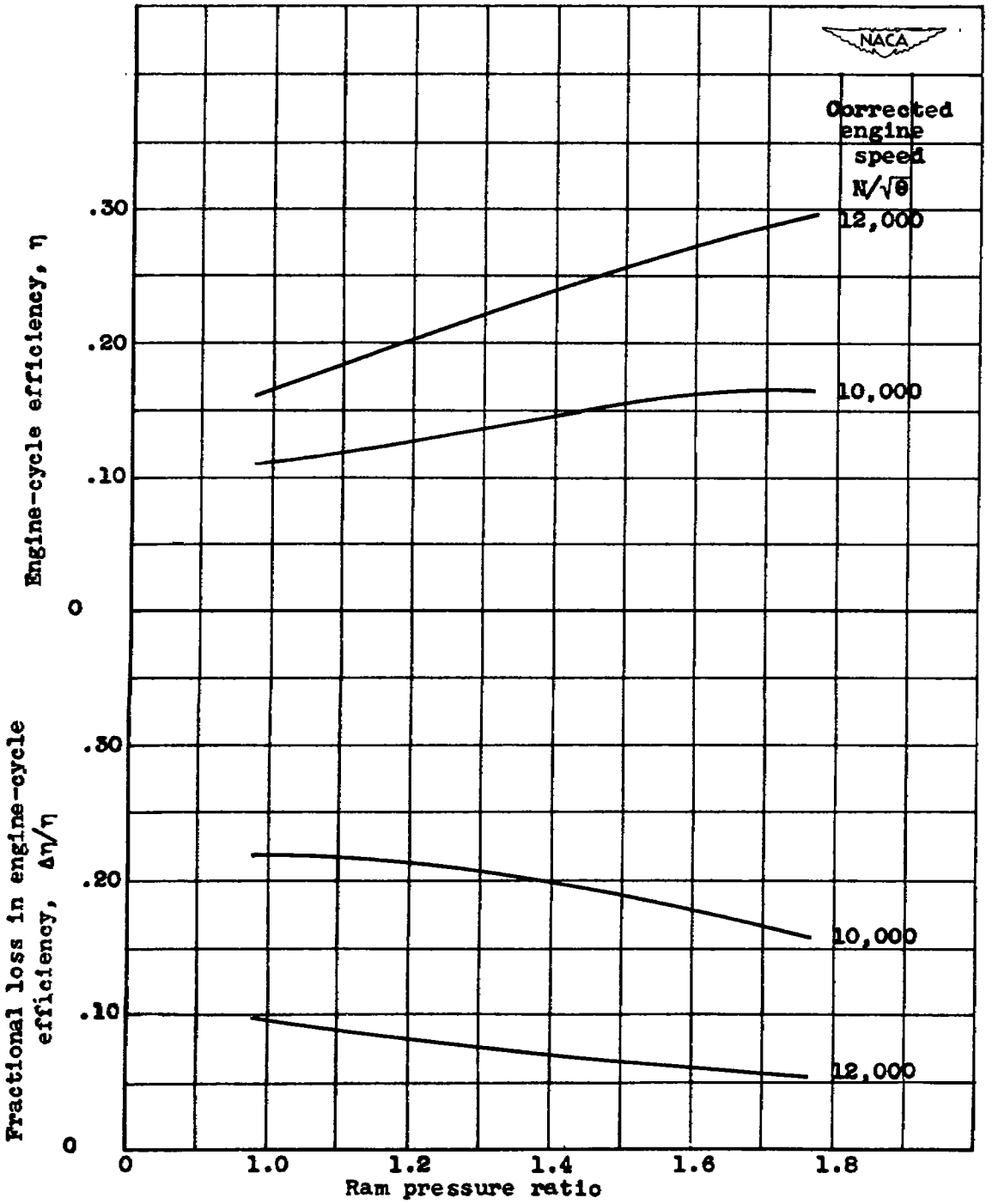

Figure 13.- Variation with ram-pressure ratio of engine-cycle efficiency and fractional loss in engine-cycle efficiency due to combustion-chamber pressure losses of type C combustion chamber for constant values of corrected engine speed at simulated altitude of 30,000 feet.